

Synthesis, Spectroscopy, and Catalytic Properties of Cationic Organozirconium Adsorbates on "Super Acidic" Sulfated Alumina. "Single-Site" Heterogeneous Catalysts with Virtually 100% Active Sites

Christopher P. Nicholas, Hongsang Ahn, and Tobin J. Marks*

Contribution from the Department of Chemistry, Northwestern University,
Evanston, Illinois 60208-3113

Received September 30, 2002; E-mail: t-marks@northwestern.edu

Abstract: Sulfated alumina (AIS), a highly Brønsted acidic sulfated metal oxide, is prepared by the impregnation of γ -alumina with 1.6 M H_2SO_4 , followed by calcination at 550 °C for 3 h. ^{13}C CPMAS NMR spectroscopy of the chemisorbed $^{13}\text{C}_\alpha$ -enriched organozirconium hydrocarbyl $\text{Cp}'_2\text{Zr}(^{13}\text{CH}_3)_2$ (**2***)/AIS ($\text{Cp}' = \eta^5\text{-(CH}_3)_5\text{C}_5$) reveals that the chemisorption process involves M–C σ -bond protonolysis at the strong surface Brønsted acid surface sites to yield a "cation-like" highly reactive zirconocenium electrophile, $\text{Cp}'_2\text{-Zr}^{13}\text{CH}_3^+$. In contrast, chemisorption of **2*** on dehydroxylated alumina (DA) yields a similar cation via methide transfer to surface Lewis acid sites, while chemisorption onto dehydroxylated silica yields a μ -oxo $\text{Cp}'_2\text{-Zr}(^{13}\text{CH}_3)\text{-OSi}\equiv$ species. Two complementary active site kinetic assays for benzene hydrogenation show that, unlike typical heterogeneous and supported organometallic catalysts, $97 \pm 2\%$ of all $\text{Cp}'_2\text{ZrMe}_3$ (**3**)/AIS sites are catalytically significant, demonstrating that the species identified by ^{13}C CPMAS NMR is indeed the active species. **3**/AIS mediates benzene hydrogenation with a turnover frequency of 360 h^{-1} at 25 °C/1.0 atm H_2 . Active site assays were also conducted for ethylene polymerization and reveal that 87 \pm 3% of **3**/AIS sites are catalytically active, again demonstrating that nearly all zirconium sites are catalytically significant. Relative rates of ethylene homopolymerization mediated by the catalysts prepared via $\text{Cp}_2\text{Zr}(\text{CH}_3)_2$ (**1**), $\text{Cp}'_2\text{Zr}(\text{CH}_3)_2$ (**2**), $\text{Cp}'\text{Zr}(\text{CH}_3)_3$ (**3**), $\text{Zr}(\text{CH}_2\text{TMS})_4$ (**4**), and $\text{Zr}(\text{CH}_2\text{Ph})_4$ (**5**) ($\text{Cp} = \eta^5\text{-C}_5\text{H}_5$) chemisorption on AIS are $5/\text{AIS} \geq 4/\text{AIS} \geq 3/\text{AIS} > 2/\text{AIS} \geq 1/\text{AIS}$ for ethylene homopolymerization at 150 psi C_2H_4 , 60 °C. Under identical conditions, the polymerization rate for **3**/DA is $\sim 1/10$ that for **3**/AIS.

Introduction

Chemisorption of discrete metal-organic complexes on metal oxide surfaces has been shown to yield molecular adsorbates with exceptional catalytic activities in a variety of hydrocarbon transformations¹ and olefin polymerization processes.² In a

number of cases, the structural nature of these adsorbates has been studied by various combinations of magnetic resonance, vibrational, and X-ray spectroscopies, as well as by evolved product analysis. While such studies have provided an informative picture of the surface chemisorption/coordination chemistry, their link to the *actual catalytic species* remains tenuous, because the percentage of sites which are catalytically significant has in most cases remained undefined and is likely to be small.^{3,4a-c,e,f} In previous research, we employed ^{13}C -enriched organoactinides and early transition metal hydrocarbyls as model adsorbates and studied their chemisorptive reaction pathways on various metal oxide surfaces.^{4,5} It was demonstrated that intrinsically strong

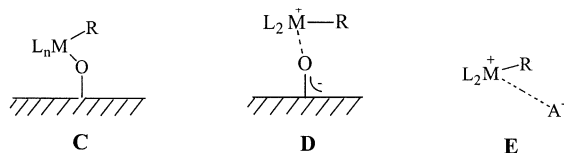
- (1) (a) Sheldon, R. A.; van Bekkum, H., Eds. *Fine Chemicals through Heterogeneous Catalysis*; Wiley-VCH: Weinheim, 2001. (b) Lindner, E.; Auer, F.; Baumann, A.; Wegner, P.; Mayer, H. A.; Bertagnolli, H.; Reinohl, U.; Ertel, T. S.; Weber, A. *J. Mol. Catal. A: Chem.* **2000**, *157*, 97–109. (c) Lefebvre, F.; Basset, J. M. *J. Mol. Catal. A: Chem.* **1999**, *146*, 3–12. (d) Scott, S. L.; Basset, J.-M.; Niccolai, G. P.; Santini, C. C.; Candy, J. P.; Lecuyer, C.; Quignard, F.; Choplin, A. *New J. Chem.* **1994**, *18*, 115–122. (e) Iwasawa, Y.; Gates, B. C. *CHEMTECH* **1989**, *3*, 173–181 and references therein. (f) Basset, J.-M., et al., Eds. *Surface Organometallic Chemistry: Molecular Approaches to Surface Catalysis*; Kluwer: Dordrecht, 1988. (g) Iwasawa, Y. *Adv. Catal.* **1987**, *35*, 187–264.
- (2) (a) Gladysz, J. A., Ed. *Chem. Rev.* **2000**, *100* (special issue on "Frontiers in Metal-Catalyzed Polymerization"). (b) Marks, T. J.; Stevens, J. C., Eds. *Top. Catal.* **1999**, *7*, 1 (special volume on "Advances in Polymerization Catalysis. Catalysts and Processes"). (c) Kaminsky, W. *Metalorganic Catalysts for Synthesis and Polymerization: Recent Results by Ziegler-Natta and Metallocene Investigations*; Springer-Verlag: Berlin, 1999. (d) Britovsek, G. J. P.; Gibson, V. C.; Wass, D. F. *Angew. Chem., Int. Ed.* **1999**, *38*, 428–447. (e) Jordan, R. F. *J. Mol. Catal.* **1998**, *128* (special issue on "Metallocene and Single Site Olefin Catalysis") and references therein. (f) Kaminsky, W.; Arndt, M. *Adv. Polym. Sci.* **1997**, *127*, 144–187. (g) Bochmann, M. *J. Chem. Soc., Dalton Trans.* **1996**, 255–270. (h) Brintzinger, H. H.; Fischer, D.; Müllhaupt, R.; Rieger, B.; Waymouth, R. M. *Angew. Chem., Int. Ed. Engl.* **1995**, *34*, 1143–1170. (i) Soga, K.; Terano, M., Eds. *Catalyst Design for Tailor-Made Polyolefins*; Elsevier: Tokyo, 1994.

- (3) (a) Kotrel, S.; Rosynek, M. P.; Lunsford, J. H. *J. Catal.* **1999**, *182*, 278–81. (b) Weddle, K. S.; Aiken, J. D., III; Finke, R. G. *J. Am. Chem. Soc.* **1998**, *120*, 5653–66. (c) Fu, S.-L.; Rosynek, M. P.; Lunsford, J. H. *Langmuir* **1991**, *7*, 1179–87 and references therein.
- (4) (a) Eisen, M. S.; Marks, T. J. *J. Mol. Catal.* **1994**, *86*, 23–50. (b) Marks, T. J. *Acc. Chem. Res.* **1992**, *25*, 57–65. (c) Eisen, M. S.; Marks, T. J. *J. Am. Chem. Soc.* **1992**, *114*, 10358–10368. (d) Finch, W. C.; Gillespie, R. D.; Hedden, D.; Marks, T. J. *J. Am. Chem. Soc.* **1990**, *112*, 6221–6232. (e) Gillespie, R. D.; Burwell, R. L., Jr.; Marks, T. J. *Langmuir* **1990**, *6*, 1465–1477. (f) Dahmen, K. H.; Hedden, D.; Burwell, R. L., Jr.; Marks, T. J. *Langmuir* **1988**, *4*, 1212–1214. (g) Toscano, P. J.; Marks, T. J. *J. Am. Chem. Soc.* **1985**, *107*, 653–659. (h) He, M.-Y.; Xiong, G.; Toscano, P. J.; Burwell, R. L., Jr.; Marks, T. J. *J. Am. Chem. Soc.* **1985**, *107*, 641–652.
- (5) (a) Ahn, H.; Marks, T. J. *J. Am. Chem. Soc.* **2002**, *124*, 7103–10. (b) Toscano, P. J.; Marks, T. J. *Langmuir* **1986**, *2*, 820–823.

Lewis acidic surfaces such as highly dehydroxylated alumina (DA), partially dehydroxylated alumina (PDA), and MgCl_2 can activate metallocenes and related hydrocarbyls via heterolytic M–C bond scission, transferring an alkide group to surface acid sites and forming “cationic” structures (e.g., structure **A**).⁴ This



structural model is strongly supported by the synthesis, isolation, and structural characterization of single-crystal molecular analogues (e.g., structure **B** where **A** = organo-Lewis acid).⁶ However, the percentage of catalytically significant metal sites for olefin hydrogenation on these surfaces was shown to be only ~8% on DA (accompanied by high catalytic activity) and ~50% on MgCl_2 (accompanied by modest activity) by kinetic poisoning experiments. It was also established that metal hydrocarbyl chemisorption on conventional weakly Brønsted acidic surfaces such as partially dehydroxylated silica (PDS) and MgO yields catalytically less active “ μ -oxo” structures via M-CH₃ protonolysis (e.g., structure **C**).^{4b,d,g,5} Here the strong oxo conjugate



base of the weak surface Brønsted acid strongly coordinates to the cationic metal center. In marked contrast, recent studies of group 4 metallocene hydrocarbyls supported on sulfated zirconia (ZrS)⁷ reveal that organoactinide and organo-group 4 complexes undergo facile M–C σ -bond protonolysis at the strong surface Brønsted acid sites to yield highly reactive “cation-like” organometallic electrophiles (proposed structure **D**). This reactivity mode finds analogy in the solution phase protonolytic activation of metallocene alkyls by cocatalysts such as $\text{ArNMe}_2\text{H}^+\text{B}(\text{C}_6\text{F}_5)_4^-$ (e.g., structure **E** where $\text{A}^- = \text{B}(\text{C}_6\text{F}_5)_4^-$).^{6a,8} For $\text{Cp}'\text{Zr}(\text{CH}_3)_3/\text{ZrS}$ ($\text{Cp}' = \eta^5\text{-}(\text{CH}_3)_5\text{C}_5$), the percentage of sites active for benzene hydrogenation is ~65%.

In addition to sulfated zirconia,⁹ which is thought to be one of the most “superacidic” high surface area oxides known, other

sulfate-modified metal oxide catalysts¹⁰ such as sulfated Al_2O_3 ,¹¹ SiO_2 ,¹² SnO_2 ,¹³ Fe_2O_3 ,¹⁴ TiO_2 ,¹⁵ and HfO_2 ¹⁶ have received considerable attention because sulfate modification frequently induces significant activity enhancement for hydrocarbon skeletal rearrangements and is usually accompanied by surface functional group and morphological changes. In this respect, alumina is of particular interest due to its enormous importance as a high-surface area support in industrial catalysis and for comparison to our chemisorption studies on DA. In this contribution, we report on the chemisorptive properties of several classes of organozirconium hydrocarbyls on sulfated γ -alumina (AIS), characterize the surface chemistry by high-resolution ¹³C CPMAS NMR spectroscopy, assess the catalytic activities with respect to benzene hydrogenation as well as ethylene homopolymerization, and perform kinetic active site counting measurements. The latter reveal, via several complementary assay techniques, an unprecedented level of catalytically significant sites. We show that highly electrophilic, “cation-like” organozirconium species are formed on AIS and that such species exhibit high olefin polymerization activity, as well as appreciable benzene hydrogenation activity.¹⁷

Experimental Section

All procedures were performed in Schlenk-type glassware interfaced to a high-vacuum (10^{-5} – 10^{-6} Torr) line or in a nitrogen-filled Vacuum Atmospheres glovebox (0.5–1 ppm O₂). Argon (Matheson) was purified by passage through MnO/vermiculite and Davison 4A molecular sieve columns. Oxygen (Matheson) was dried by passage through Drierite (Hammond Co.). Ethylene (Matheson) was purified by passage through an oxygen/moisture trap (Matheson, model 6427-2S). All solvents were distilled from Na/K alloy. The organometallic complexes $\text{Cp}_2\text{Zr}(\text{CH}_3)_2$ (**1**),¹⁸ $\text{Cp}'_2\text{Zr}(\text{CH}_3)_2$ (**2**),¹⁹ $\text{Cp}'\text{Zr}(\text{CH}_3)_3$ (**3**)²⁰ [$\text{Cp} = \eta^5\text{-C}_5\text{H}_5$, $\text{Cp}' = \eta^5\text{-}(\text{CH}_3)_5\text{C}_5$], $\text{Zr}(\text{CH}_2\text{TMS})_4$ (**4**)²¹ [$\text{TMS} = \text{Si}(\text{CH}_3)_3$], and $\text{Zr}(\text{CH}_2\text{Ph})_4$ (**5**)²² were prepared by the literature procedures. The labeled complex, $\text{Cp}'_2\text{Zr}(\text{CH}_3)_2$ (**2***), was synthesized from ¹³CH₃Li·LiI prepared from ¹³CH₃I (99% ¹³C, Cambridge Isotopes) using analogous methods. Highly dehydroxylated silica (DS) was prepared from Davison grade 62 silica gel (60–80 mesh, previously washed with 0.1 M HNO₃, and dried) by calcining it in a stream of CO (flow rate = 100 mL/min) at 950 °C for 1 h, calcining it in a stream of Ar (flow rate = 100 mL/min) at 950 °C, and, finally, heating it under high vacuum (5×10^{-6} Torr) at 800

- (6) (a) Chen, E. Y.-X.; Marks, T. J. *J. Chem. Rev.* **2000**, *100*, 1391–1434 and references therein. (b) Chen, Y.-X.; Metz, M. V.; Li, L.; Stern, C. L.; Marks, T. J. *J. Am. Chem. Soc.* **1998**, *120*, 6287–6305. (c) Deck, P. A.; Beswick, P. A.; Marks, T. J. *J. Am. Chem. Soc.* **1998**, *120*, 1772–1784. (d) Sun, Y.; Spence, R. E. V. H.; Piers, W. E.; Parvez, M.; Yap, G. P. A. *J. Am. Chem. Soc.* **1997**, *119*, 5132–5143 and references therein. (e) Baumann, R.; Davis, W. M.; Schrock, R. R. *J. Am. Chem. Soc.* **1997**, *119*, 3830–3831. (f) Wang, Q.; Gillis, D. J.; Quyoum, R.; Jeremic, D.; Tidoret, M.-J.; Baird, M. C. *J. Organomet. Chem.* **1997**, *527*, 7–14. (g) Chen, Y.-X.; Stern, C. L.; Yang, S.; Marks, T. J. *J. Am. Chem. Soc.* **1996**, *118*, 12451–12452. (h) Yang, X.; Stern, C. L.; Marks, T. J. *J. Am. Chem. Soc.* **1994**, *116*, 10015–10031. (7) (a) Ahn, H.; Nicholas, C. P.; Marks, T. J. *Organometallics* **2002**, *21*, 1788–1806. (b) Ahn, H.; Marks, T. J. *J. Am. Chem. Soc.* **1998**, *120*, 13533–13534. (8) (a) Chen, Y.-X.; Metz, M. V.; Li, L.; Stern, C. L.; Marks, T. J. *J. Am. Chem. Soc.* **1998**, *120*, 6287–6305. (b) Jia, L.; Yang, X.; Stern, C. L.; Marks, T. J. *Organometallics* **1997**, *16*, 842–857. (c) Giardello, M. A.; Eisen, M. S.; Stern, C. L.; Marks, T. J. *J. Am. Chem. Soc.* **1995**, *117*, 12114–12129. (d) Jia, L.; Yang, X.; Stern, C. L.; Marks, T. J. *Organometallics* **1994**, *13*, 3755–3757. (e) Hlatky, G. G.; Eckman, R. R.; Turner, H. W. *Organometallics* **1992**, *11*, 1413–1416. (f) Yang, X.; Stern, C. L.; Marks, T. J. *Organometallics* **1991**, *10*, 840–842. (g) Turner, H. W.; Hlatky, G. G. *PCT Int. Appl. WO 88/05793* (Eur. Pat. Appl. EP 211004, 1988). (9) For recent reviews on solid acids, see: (a) Song, X.; Sayari, A. *Catal. Rev.-Sci. Eng.* **1996**, *38*, 329–412 and references therein. (b) Corma, A. *Chem. Rev.* **1995**, *95*, 559–614. (c) Yamaguchi, T. *Appl. Catal.* **1990**, *61*, 1–25.

- (10) (a) Matsuhashi, H.; Motoi, H.; Arata, K. *Catal. Lett.* **1994**, *26*, 325–328. (b) Arata, K. *Adv. Catal.* **1990**, *37*, 165–211. (11) (a) Escalona, P. E.; Penarroya, M. M.; Morterra, C. *Langmuir* **1999**, *15*, 5079–5087. (b) Yang, T.; Chang, T.; Yeh, C. *J. Mol. Catal. A: Chem.* **1997**, *123*, 163–169. (c) Yang, T.; Chang, T.; Yeh, C. *J. Mol. Catal. A: Chem.* **1997**, *115*, 339–346. (d) Arata, K.; Hino, M. *Appl. Catal.* **1990**, *59*, 197–204. (e) Przystajko, W.; Fiedorow, R.; Dalla Lana, I. G. *Appl. Catal.* **1985**, *15*, 265–275. (12) Matsuhashi, H.; Hino, M.; Arata, K. *Catal. Lett.* **1991**, *8*, 269–272. (13) (a) Chavan, S.; Zubaidha, P. K.; Dantale, S. W.; Keshavaraja, A.; Ramaswamy, A. V.; Ravindranathan, T. *Tetrahedron Lett.* **1996**, *37*, 233–236. (b) Matsuhashi, H.; Hino, M.; Arata, K. *Appl. Catal.* **1990**, *59*, 205–212. (c) Matsuhashi, H.; Hino, M.; Arata, K. *Chem. Lett.* **1988**, 1027–1028. (14) Hino, M.; Arata, K. *Chem. Lett.* **1979**, 477–480. (15) (a) Chen, J. P.; Yang, R. T. *Catal.* **1993**, *139*, 277–288. (b) Hino, M.; Arata, K. *J. Chem. Soc., Chem. Commun.* **1979**, 1148–1149. (16) Arata, K.; Hino, M. *React. Kinet. Catal. Lett.* **1984**, *25*, 143–145. (17) These results communicated in part: Marks, T. J.; Nicholas, C. P.; Ahn, H. Abstracts of Papers, 224th ACS National Meeting, Boston, MA, August 18–22, 2002; INOR-635. (18) Wailes, P. C.; Weigold, H.; Bell, A. P. *J. Organomet. Chem.* **1972**, *34*, 105–164. (19) Manriquez, J. M.; McAlister, D. R.; Sanner, R. D.; Bercaw, J. E. *J. Am. Chem. Soc.* **1978**, *100*, 2716–2724. (20) Wolczanski, P. T.; Bercaw, J. E. *Organometallics* **1982**, *1*, 793–799. (21) Collier, M. R.; Lappert, M. F.; Pearce, R. *J. Chem. Soc., Dalton Trans.* **1973**, 445–451. (22) Zucchini, U.; Albizzati, E.; Giannini, U. *J. Organomet. Chem.* **1971**, *26*, 357–372.

°C for 15 h.⁵ Dehydroxylated alumina (DA, American Cyanamid γ -alumina, 99.99% purity) was prepared as previously described.^{4e,h}

Physical and Analytical Measurements. The following instruments were used in this study: ¹H, ¹³C NMR (Varian Mercury 400 and Varian INOVA 500), ¹³C CP/MAS solid-state NMR (Varian VXR300), BET/pore size distribution (Omnisorb 360), ICP (Thermo Jarrell Ash), GC/MSD (Hewlett-Packard 6890), and IR (Biorad FTS-60). ¹H and ¹³C NMR experiments on air-sensitive solution samples were conducted in Teflon valve-sealed sample tubes (J-Young). For ¹³C CP/MAS solid-state NMR spectroscopy, air-sensitive samples were loaded into cylindrical silicon nitride rotors in the glovebox with O-ring sealed Kel-F caps. Typically, spinning rates of ≥ 6.2 kHz could be achieved with the Doty Scientific 5 mm supersonic probe using boil-off nitrogen as the spinning gas to prevent sample exposure to air. Because the samples are extremely air- and moisture-sensitive, rotors were loaded and packed with catalyst samples inside the glovebox under an anaerobic nitrogen atmosphere. For routine spectra of organozirconium adsorbates, the optimum cross-polarization contact time was found to be 0.55–0.86 ms, and the optimum recycle time was found to be 4–6 s. The ¹³C 90° pulse width and the Hartmann–Hann condition were determined by a parameter-arrayed experiment for each measurement. In general, 2700–10 000 scans were required to obtain satisfactory spectra of the supported organometallic samples.

Preparation of Sulfated Alumina (AIS). Using a modification of a literature procedure,^{11b} we impregnated 2.0 g of γ -alumina (American Cyanamid, BET surface area = 94 m²/g) with 20 mL of 1.6 M H₂SO₄.^{11c} After being stirred 30 min, the slurry was filtered, and the solid was dried at 120 °C for 18 h. Next, the sample was crushed, sieved to mesh 60–80, and subsequently calcined at 550 °C for 3 h in flowing O₂ (100 mL/min). Finally, the sulfated alumina was activated under high vacuum (5×10^{-6} Torr) at 450 °C for 15 min and stored under a dry N₂ atmosphere. A sample of this sulfated metal oxide was analyzed by BET techniques (N₂ desorption) using an Omnisorb 360 instrument, which showed the sulfated alumina to have a surface area of 94 m²/g and a most frequent pore size of 2.5 nm.

Chemisorption of Organometallic Complexes on Prepared Supports. In a two-sided fritted reaction vessel interfaced to the high-vacuum line, 10 mL of pentane was condensed onto well-mixed, measured quantities of the organometallic complex and support. The resulting slurry was next stirred for 45 min and filtered. The impregnated support was collected on the frit, washed three times with pentane, and finally dried in vacuo for 30 min. When a sample synthesized in this manner was analyzed by ICP spectroscopy following digestion with 48% HF, 0.25 Zr atom/nm² (3.9×10^{-8} mol Zr/mg AIS) and 3.02 S atom/nm² were the maximum quantities of metal hydrocarbyl and sulfur present. If more than the maximum coverage of organozirconium precatalyst is used, excess reagent is visible in the other end of the fritted vessel after the pentane evaporation. The prepared catalysts were stored under a dry N₂ atmosphere at –40 °C until used.

Benzene Hydrogenation Experiments. Catalytic hydrogenation studies were performed with two different types of reactor as described below.

Reactor A. A glass reaction vessel (~10 mL in volume) with Morton-type indentations was fitted with a high-speed vortex agitator (American Scientific MT-51 vortex mixer) to ensure efficient mixing, a water jacket connected to a recirculating pump, a Haake constant-temperature bath (25.0(1) °C), calibrated burets for the addition of reagents, and a large diameter flexible stainless steel connection to a high-vacuum line. The consumption of H₂ was measured with an Omega PX425-300GV digital pressure transducer.

In a typical experiment, the reaction vessel was dried under high vacuum (5×10^{-7} Torr) for >2 h prior to experimentation. In the glovebox, the reaction chamber was charged with catalyst, and the burets were loaded with substrate/poison. The vessel was then transferred to the vacuum line, evacuated, and filled with H₂ (1.0 atm). The thermostated water circulating system was then connected and

actuated. Next, 1.0 mL of substrate was introduced after waiting 5 min for equilibration. Vortex mixing was then initiated (>2000 rpm), and the H₂ pressure was recorded as a function of time.

Reactor B. In a typical experiment, a 60 mL Griffin–Worden quartz medium-pressure reactor (Kontes Corp., Vineland, NJ), connected to a 500 mL metal gas ballast tank, was flamed under high vacuum and charged in the glovebox with 50 mg of supported catalyst and 1.0 mL (1.1×10^{-2} mol) of benzene dried over Na/K. The apparatus was removed from the glovebox and attached to the high-vacuum line. After thorough evacuation (10^{-5} Torr) of the reactor at –78 °C, the reactor was warmed to room temperature and pressurized to 1.0 atm of H₂. The reactor was then immersed in an oil bath maintained at 25(0.1) °C and stirred rapidly (>1500 rpm). The consumption of H₂ was measured with an Omega PX425-300GV digital pressure transducer.

Ethylene Homopolymerization Experiments. The supported catalyst was charged into reactor B along with 2.5 mL of dry toluene. The reactor was then degassed at –78 °C, after which time the reactor was immersed in an oil bath maintained at 60 °C and charged with ethylene to the desired pressure, and the slurry was rapidly stirred. After 15 min, the polymerization was quenched with methanol, and the polymeric product was collected by filtration, dried overnight under high vacuum at 80 °C, and weighed.

Active Site Counting Experiments. A 9.338×10^{-4} M solution of H₂O in C₆H₆ was prepared by thoroughly drying 935.03 g of benzene over Na/K and vacuum transferring to a separate flask where 18 μ L of H₂O was syringed in under an Ar flush. This solution was then used in poisoning experiments. Additionally, to investigate the effect of other poisons, a 3.762×10^{-4} M solution of neopentyl alcohol in benzene was prepared by twice vacuum subliming the neopentyl alcohol to purify it, followed by adding 29.9 mg (3.39×10^{-4} mol) of it to 790.22 g (0.9016 L) of benzene. This solution was used for a batch poisoning study of olefin polymerization active sites. Active site counting was carried out in reactor A during benzene hydrogenation by titration, and in reactor B in a batchwise fashion for both benzene hydrogenation and ethylene polymerization. Titration experiments were carried out in the same manner as the catalytic hydrogenation reactions in reactor A. The catalyst was introduced into the reactor in the glovebox, followed by removal from the glovebox and evacuation on the high-vacuum line. Next, 1.0 atm of hydrogen was introduced before 1.0 mL of substrate solution was titrated in. After the hydrogenation rate was monitored for 20 min, a measured quantity of poison solution (typically 0.4 mL) was titrated in as substoichiometric aliquots, and the consumption of H₂ was monitored for 15–30 min before another aliquot was titrated in.

Batch poisoning experiments using benzene hydrogenation as the test reaction were carried out by injecting measured quantities of degassed H₂O in C₆D₆ directly into reactor B during the hydrogenation process, followed by measuring the catalytic activity. Batch poisoning experiments using ethylene polymerization as the test reaction were carried out in a manner similar to that described above. In place of the 2.5 mL of toluene usually added to the reactor during ethylene polymerization experiments, substoichiometric aliquots of poison solution (either H₂O or NpOH) were added with enough toluene to maintain the solvent volume at a constant 2.5 mL. The usual ethylene polymerization conditions were then followed. The percentage of active sites was determined by measuring the activity, and then plotting the activities as a function of added poison, calculating the linear least-squares best fit line for the data and extrapolating to the zero activity point.

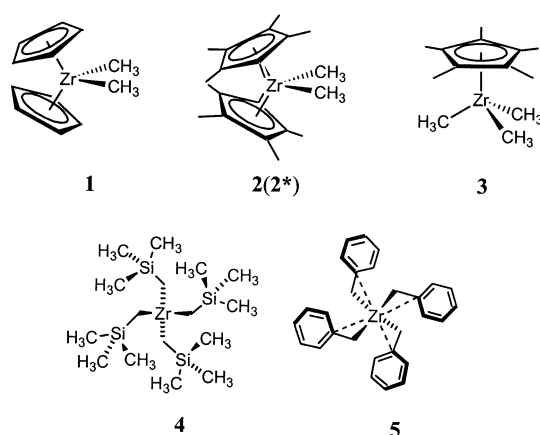
In all cases, active site calculations are based on the assumption that each molecule of either H₂O or NpOH reacts with/poisons one active catalytic site.

Results and Discussion

This section begins with a discussion of the chemisorptive syntheses of the heterogeneous catalysts derived from orga-

nozirconium precursors and the support of interest, sulfated alumina (AIS). We then discuss the structural characteristics of $\text{Cp}'_2\text{Zr}(\text{CH}_3)_2$ ($\mathbf{2}^*$) as a probe molecule supported on AIS vis-à-vis the results for $\mathbf{2}^*$ supported on DS (dehydroxylated silica) and DA (dehydroxylated alumina) as deduced by ^{13}C CPMAS NMR spectroscopy. Third, benzene hydrogenation mediated by $\mathbf{3}/\text{AIS}$ as well as active site counting experiments will be discussed. Last, we investigate the ethylene homopolymerization properties of a selected group of AIS-supported organozirconium hydrocarbyls that offer variations in cyclopentadienyl ligand substitution as well as in number and type of hydrocarbyl ligands.

Catalyst Syntheses. All organometallic catalyst precursors used in this study were prepared as described elsewhere.^{18–22} To examine the effects of precatalyst ancillary ligation on the catalytic properties, bis(cyclopentadienyl) ($\mathbf{1}$, $\mathbf{2}$), mono(cyclopentadienyl) ($\mathbf{3}$), and homoleptic hydrocarbyl ($\mathbf{4}$, $\mathbf{5}$) zirconium complexes were employed as adsorbates on sulfated alumina (AIS). AIS prepared as described in the Experimental Section



has been reported to exhibit “superacidic” reactivity patterns such as rapid hydrocarbon skeletal isomerization^{11b} and benzoylation.^{11d}

Structural Characterization of Adsorbate Species. Organometallic molecule adsorption chemistry on AIS was examined by solid-state ^{13}C CPMAS NMR techniques using the labeled probe complex $\mathbf{2}^*$, $\text{Cp}'_2\text{Zr}(\text{CH}_3)_2$, and comparing/contrasting the fate of the ^{13}C labeled methyl group, originally coordinated to Zr, with that of $\mathbf{2}^*$ on DS and DA (Figure 1). We desired to use complexes derived from complex $\mathbf{3}^*$, but due to the lower coordinative saturation of complex $\mathbf{3}^*$, $\mathbf{3}^*/\text{AIS}$ decomposes in the NMR in the time necessary to obtain a meaningfully resolved solid-state CPMAS NMR (overnight). In Figure 1A, the ^{13}C CPMAS spectrum of $\mathbf{2}^*/\text{DS}$ exhibits resonances at δ 119.0, 31.0, 9.0, and -6.0 . The resonances at δ 119 and 9.0 are readily assigned to Cp ring carbons and Cp-CH₃ carbons, respectively, in analogy to solution phase NMR data (e.g., δ 117.4 and 12.1 for $\text{Cp}'_2\text{Zr}(\text{CH}_3)_2$; Table 1). The weak resonance at δ -6.0 is assigned to a surface Si-CH₃ functionality in close analogy to the Si-CH₃ signal at δ -5.4 of $\text{Cp}'_2\text{Th}(\text{CH}_3)_2/\text{DS}$, which forms via Si-O bond cleavage to form a μ -oxo species (eq 1).^{5a} The major resonance for $\text{Cp}'_2\text{Zr}(\text{CH}_3)_2/\text{DS}$ appears at relatively high field, δ 31.0, and strongly supports the same reaction mode for $\mathbf{2}^*$ to form Si- ^{13}C H₃ and $\text{Cp}'_2\text{Zr}(\text{CH}_3)\text{OSi}\equiv$ species. This

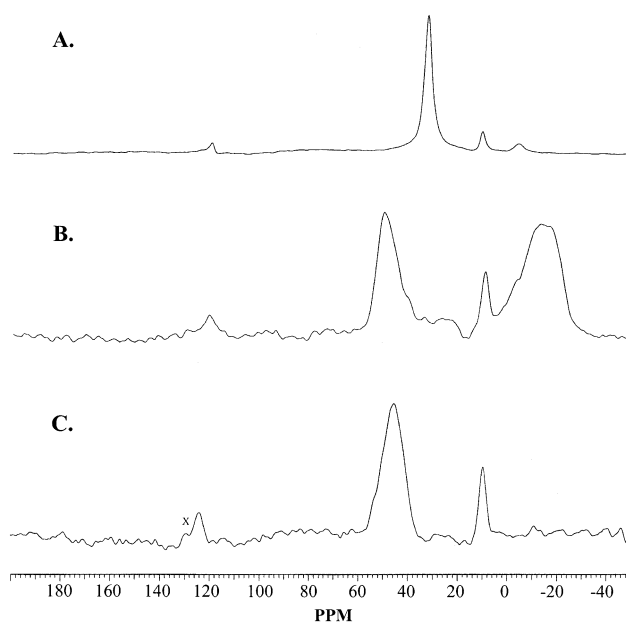
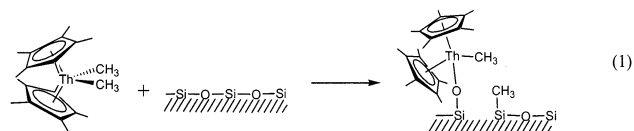


Figure 1. ^{13}C CPMAS NMR spectra (75.4 MHz) of (A) $\text{Cp}'_2\text{Zr}(\text{CH}_3)_2$ - $\mathbf{2}^*/\text{DS}$ (3000 scans, repetition time = 6.0 s, contact time = 0.55 ms, spinning speed = 6.3 kHz), (B) $\mathbf{2}^*/\text{DA}$ (2700 scans, repetition time = 4 s, contact time = 0.55 ms, spinning speed = 6.2 kHz), and (C) $\mathbf{2}^*/\text{AIS}$ (9850 scans, repetition time = 4 s, contact time = 0.55 ms, spinning speed = 6.3 kHz) (x = spinning sideband).

Table 1. Solid-State ^{13}C NMR Chemical Shift Data for Neat and Supported Organometallic Complexes^a

complex ^b	Cp' ring	M- $^{13}\text{C}_\alpha$	Cp'-CH ₃	others
$\text{Cp}'_2\text{Zr}(\text{CH}_3)_2$ ($\mathbf{2}^*$) ^c	117.4	36.8	12.1	
$\mathbf{2}^*/\text{DS}$	119.0	31.5	9.0	-6.0 (Si-CH ₃)
$\mathbf{2}^*/\text{DA}$	121.0	49.2	9.1	-12.8 (Al-CH ₃)
$\mathbf{2}^*/\text{AIS}$	123.0	46.0	9.6	

^a In ppm downfield from Me_4Si , referenced to the solid-state ^{13}C spectrum of adamantane (see Experimental Section for details). ^b Cp' = η^5 -(CH₃)₅C₅; DS = highly dehydroxylated silica; DA = highly dehydroxylated alumina; AIS = sulfated alumina. ^c Measured in C_6D_6 solution.



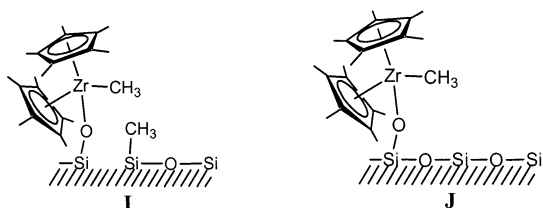
assignment (structure **I**)²³ is supported by data for well-characterized homogeneous analogues such as $\text{Cp}'_2\text{Zr}(\text{CH}_3)\text{OR}$ [δ 27.9, R = CH₂CH₂SPh].²⁴ The relative Si- ^{13}C :Zr- ^{13}C intensities suggest that Zr-CH₃ protonolysis via residual surface Si-OH groups²⁵ to yield a structure such as **J** is the predominant chemisorptive process. As expected from the poorly electrophilic character of such species,^{4b,f,g,5} compound $\mathbf{2}^*/\text{DS}$ exhibits marginal olefin polymerization and hydrogenation activity.

In Figure 1B, the ^{13}C CPMAS NMR spectrum of $\mathbf{2}^*/\text{DA}$ exhibits four resonances at δ 121.0, 49.3, 9.1, and -12.8 .^{4e} The two bands at δ 121.0 and 9.1 are straightforwardly assigned to Cp ring carbons and Cp-CH₃ carbons, analogous to the case

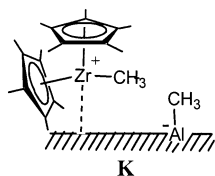
(23) Because the Si- ^{13}C H₃ signal (δ -6.0) is relatively weak as compared to the Zr- ^{13}C H₃ resonance (δ 31.0), it cannot be totally excluded that the major chemisorption pathway involves protonolysis of complex $\mathbf{1}^*$ by residual surface silanol groups to form μ -oxo species.

(24) Fandos, R.; Hernández, C.; Otero, A.; Rodríguez, A.; Ruiz, M. J.; Terreros, P. J. *Organomet. Chem.* **2000**, *606*, 156–162.

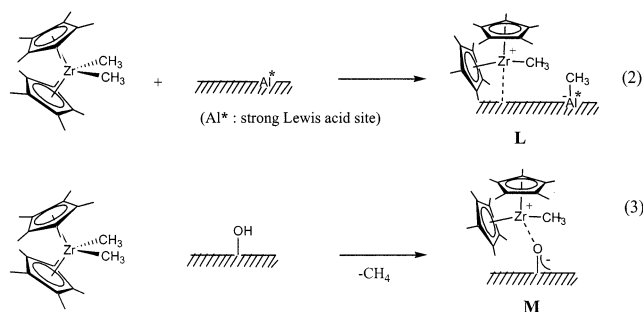
(25) Dehydroxylated silica still contains residual surface hydroxyl groups: McDaniel, M. P.; Welch, M. B. *J. Catal.* **1983**, *82*, 98–109.



of **2***/DS. An intense, broad, upfield resonance at $\delta -12.8$ can be assigned to a surface $\text{Al}-^{13}\text{CH}_3$ functionality, for example, a labeled methyl group transferred onto a DA surface Lewis acid center. Such a feature is observed in the spectra of other organo-zirconium and -actinide complexes chemisorbed on DA [e.g., $\delta -12.8$ for $\text{Cp}_2\text{Zr}(^{13}\text{CH}_3)_2/\text{DA}$ ^{4f} and $\delta -13$ for $\text{Cp}'_2\text{Th}(^{13}\text{CH}_3)_2/\text{DA}$ ^{4d,g}]. Note that a low field displacement of the $\text{Zr}-^{13}\text{CH}_3$ resonance of **1***/DA is observed ($\delta 49.2$), as compared to the data for neat **2*** or **2***/DS (Table 1). Thus, a “cation-like” electron-deficient $\text{Cp}_2\text{Zr}^{13}\text{CH}_3^+$ species is reasonably suggested, supported by the $\delta(\text{Zr}-\text{CH}_3)$ downfield shift of a well-characterized homogeneous analogue, for example, $\text{Cp}'_2\text{Zr}^{13}\text{CH}_3^+\text{Q}^-$ at $\delta 50.36$ for $\text{Q}^- = \text{CH}_3\text{B}(\text{C}_6\text{F}_5)_3^-$.^{6h} Therefore, structure **K** is suggested as the major adsorbate species for **2***/DA. Species **2***/DA was previously reported to exhibit high catalytic activities for propylene hydrogenation (0.2 s^{-1} at $-63 \text{ }^\circ\text{C}$) and ethylene polymerization,^{4f} which are in good agreement with the present structural assignment by ^{13}C CPMAS NMR spectroscopy.



While sulfated alumina has been reported to be “superacidic”, the exact structures of the acidic centers are presently unresolved. However, adsorption/desorption studies employing small probe molecules such as NH_3 ,^{11b} pyridine,^{11b} or CH_3CN ^{11a} suggest that sulfation enhances Lewis acidity as well as the strong Lewis acid site population density (the acidity of which has been explained in terms of sulfate anion inductive effects) and also creates strong Brønsted acid sites on the alumina surface. On the basis of these observations, two plausible organozirconium chemisorption pathways can be suggested as illustrated in eqs 2 and 3, and insight into the present organometallic surface chemistry of AIS is provided by ^{13}C CPMAS NMR spectroscopy.



In the spectrum of **2***/AIS (Figure 1C), signals assignable to a Cp ring carbon at $\delta 121$ and to a $\text{Cp}-\text{CH}_3$ group at $\delta 9.6$

appear in common with the spectra of **2***/DS and **2***/DA. Also noteworthy is an intense ^{13}C methyl signal in the far downfield region ($\delta 46$) which is straightforwardly assigned to a cationic $\text{Cp}'_2\text{Zr}(^{13}\text{CH}_3)^+$ species in close agreement with **2***/DA and solution phase models (vide supra).^{6h} That there is no detectable signal at $\delta 31$ argues that the formation of a μ -oxo species is at best a minor pathway (vide supra). Importantly, the intensity of the **2***/AIS $\text{Al}-^{13}\text{CH}_3$ signal is *far weaker* than that of the $\text{Zr}-\text{CH}_3$ group, in sharp contrast to **2***/DA. These results indicate that complex **2*** reacts almost exclusively via $\text{Zr}-\text{CH}_3$ protonolysis by the surface Brønsted acid sites on AIS to form cationic structure **M** (eq 3) in a way analogous to zirconium dialkyl surface chemistry on sulfated zirconia.⁷ Note that the weak conjugate bases of the strong Brønsted acid sites behave (plausibly) as “weakly coordinating” anions. Further support for this suggested protonolytic pathway comes from the observation of a methane signal ($\delta 0.15$ in C_6D_6) in the ^1H NMR spectrum during in situ slurry phase chemisorption of **2** on AIS. For α -methyl ^{13}C -enriched complex **1*** chemisorbed on weakly Brønsted acidic, partially dehydroxylated alumina (PDA; $\sim 4 \text{ OH}_{\text{surface}}/\text{nm}^2$), large quantities of μ -oxo species are observed by ^{13}C CPMAS NMR along with methane evolution arising from protonolytic $\text{Zr}-\text{CH}_3$ cleavage (structure **C**). Interestingly, however, significant surface densities of cationic species are also formed via methide transfer to the surface as evidenced by a significant $\text{Al}-\text{CH}_3$ signal (structure **A**).^{4f,28} In contrast, the present observations with AIS show that the $\text{Zr}-\text{CH}_3$ linkage reacts almost exclusively with the stronger Brønsted acid sites and virtually no methide transfer to surface Lewis acid sites is evident.

It is unlikely that the Zr center oxidation state in the present adsorbates is lower than +4 because (i) only $\sim 1 \times 10^{-4}\%$ of Zr sites in **1**/DA exist as ESR-detectable Zr (III) species after H_2 treatment,^{4g} and only ca. $3 \times 10^{-2}\%$ exist even after H_2 treatment,^{4g} and (ii) sulfated alumina is known to be a significantly more oxidizing surface than that of alumina.²⁶

Benzene Hydrogenation Experiments. Benzene hydrogenation studies employing **3**/AIS were carried out in both types of reactor described in the Experimental Section. Results were indistinguishable in the two types of reactor. The catalyst system **3**/AIS was chosen for more detailed studies because all other catalysts formed (bis-Cp type or homoleptic) displayed significantly lower hydrogenation rates, similar to trends observed in the sulfated zirconia supported system,⁶ whereas **3**/AIS is a much more active catalyst. The turnover frequency for benzene hydrogenation at $25 \text{ }^\circ\text{C}$, 1 atm H_2 was determined to be $360 \text{ (mol benzene)(mol Zr)}^{-1} \text{ h}^{-1}$. This rate is $\sim 1/3$ that of the sulfated zirconia system **3**/ZrS,⁶ which mediates benzene hydrogenation at an unprecedented rate of $960 \text{ (mol benzene)(mol Zr)}^{-1} \text{ h}^{-1}$ at $25 \text{ }^\circ\text{C}$, 1.0 atm H_2 . For comparison, other molecule-derived early transition metal silica-supported catalysts mediate benzene hydrogenation at $120 \text{ }^\circ\text{C}$, 100–120 atm H_2 with turnover frequencies of $350\text{--}1400 \text{ h}^{-1}$.²⁷ The present rate law data can be fit to zero-order response in [substrate] and

(26) (a) Przystajko, W.; Fiedorow, R.; Dalla Lana, I. G. *Appl. Catal.* **1985**, *15*, 265–275. (b) Fiedorow, R. *Bull. Acad. Pol. Sci., Ser. Sci. Chim.* **1974**, *22*, 325–331.

(27) Profilet, R. D.; Rothwell, A. P.; Rothwell, I. P. *J. Chem. Soc., Chem. Commun.* **1993**, 42–44.

(28) Jezequel, M.; Dufaud, V.; Ruiz-Garcia, M. J.; Carrillo-Hermosilla, F.; Neugebauer, U.; Niccolai, G. P.; Lefebvre, F.; Bayard, F.; Corker, J.; Fiddy, S.; Evans, J.; Broyer, J.-P.; Malinge, J.; Basset, J.-M. *J. Am. Chem. Soc.* **2001**, *123*, 3520–3540.

Table 2. Summary of Ethylene Homopolymerization Data for Organozirconium Complexes Supported on Sulfated Alumina (AIS)^a

entry	catalyst ^b	[Zr] (μmol)	reaction time (min)	PE yield (mg)	activity ^c $\times 10^5$
1.	$\text{Cp}_2\text{Zr}(\text{CH}_3)_2$ (1)/AIS	1.17	60	94	0.80
2.	$\text{Cp}'_2\text{Zr}(\text{CH}_3)_3$ (2)/AIS	1.17	60	184	1.6
3.	$\text{Cp}'\text{Zr}(\text{CH}_3)_3$ (3)/AIS	1.17	10	228	11
4.	$\text{Zr}(\text{CH}_2\text{TMS})_4$ (4)/AIS	1.17	10	241	12
5.	$\text{Zr}(\text{CH}_2\text{Ph})_4$ (5)/AIS	1.17	8	324	21

^a Carried out at 60 °C, 150 psi of ethylene, 5.0 mL of toluene. ^b Cp = $\eta^5\text{-C}_5\text{H}_5$; Cp' = $\eta^5\text{-(CH}_3)_3\text{C}_5$; AIS = sulfated alumina. ^c Units: grams of total polymer/(mol Zr·h).

first-order response in $[\text{H}_2]$ as observed previously for benzene hydrogenation mediated by **3**/ZrS⁶ and propylene hydrogenation mediated by $\text{Cp}'_2\text{ThMe}_2/\text{DA}$ ^{3b}.

Olefin Polymerization Experiments. Ethylene homopolymerization studies employing the present organozirconium catalysts supported on AIS were carried out in a high-pressure batch reactor with rapid stirring (>1500 rpm) to minimize olefin mass transport effects, at 150 psi ethylene and 60 °C. Results are summarized in Table 2. It has been reported that organozirconium complexes such as **2** and **3** supported on pure alumina exhibit moderate ethylene homopolymerization activities.^{4f,28} Under identical polymerization conditions (150 psi ethylene, 60 °C), the ethylene homopolymerization activity of **3**/AIS (1.1×10^6 g PE/mol Zr·h) is almost 10 times that of **3**/DA (1.2×10^5 g PE/mol Zr·h). Moreover, ethylene polymerization activities follow the order: $5 \geq 4 \geq 3 > 2 \geq 1$, a trend which approximately parallels decreasing coordinative saturation. Efforts to separate the polymer from the support were unsuccessful even by extracting with 1,2,4-trichlorobenzene at 140 °C. The formation of such high molecular weight polyethylene has been also reported for the ethylene polymerization mediated by related catalyst systems such as organozirconium adsorbates supported on sulfated zirconia^{7a} or alumina.²⁸ However, IR spectra of the present polymeric products as hot-pressed films exhibit all of the characteristic, intense bands of ultrahigh-molecular weight high density/linear polyethylene,²⁹ for example, $\nu(\text{CH}_2)$ at 2933–2841 cm^{-1} , $\delta(\text{CH}_2)$ at 1464 cm^{-1} , a CH_2 wagging mode at 1362 cm^{-1} , and a CH_2 rocking mode at 716 cm^{-1} , respectively.

Active Site Assays. Active site kinetic poisoning studies were carried out to determine the percentage of active sites that contribute significantly to the rate of catalytic benzene hydrogenation or olefin polymerization. In the relatively few cases where assays have been performed, most heterogeneous^{3,30} and supported homogeneous³¹ catalysts have been found to exhibit very low active site percentages. That is, most of the surface metal sites are catalytically insignificant “spectators”. For example, Ittel reports that <6% of zirconium sites in the system $\text{Zr}(\text{CH}_2\text{CMe}_2\text{Ph})_4/\text{PDA}$ are active^{31a} for olefin polymerization. Similarly, Tait and Awdza found that <20% of the zirconocene sites in a Cp_2ZrCl_2 supported on SiO_2/MAO polymerization system are catalytically significant as measured by analysis of

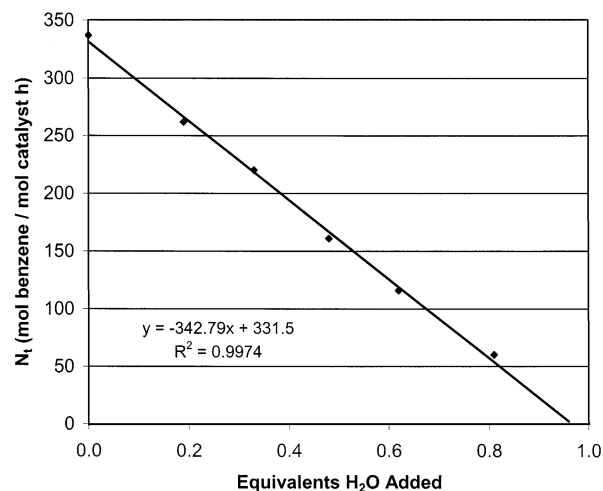


Figure 2. Plot of turnover frequency versus equivalents of added H_2O during titration poisoning of benzene hydrogenation mediated by **3**/AIS at 1.0 atm H_2 , 25 °C showing the linear best-fit line. Solving for the zero turnover point yields $97 \pm 2\%$ active sites.

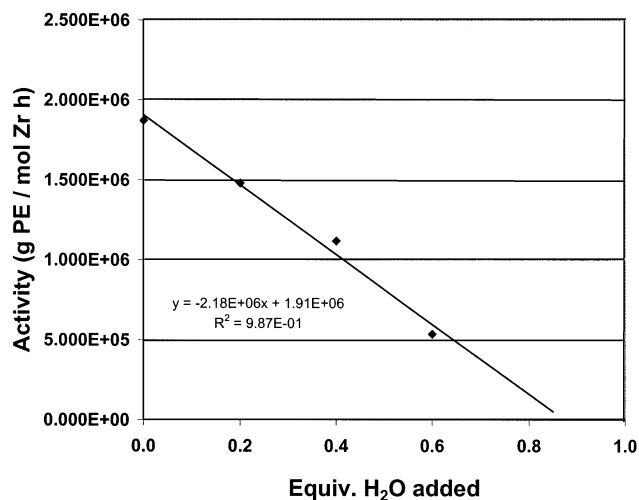


Figure 3. Plot of polymerization activity versus equivalents of added H_2O during batch poisoning of ethylene homopolymerization mediated by **3**/AIS at 150 psi ethylene, 60 °C showing the linear best-fit line. Solving for the zero turnover point yields $87 \pm 3\%$ active sites.

tritiated methyl groups generated by quenching with $^3\text{H}_3\text{COH}$.^{31b} The hope for the ideal “single-site” supported catalyst is that 100% of the sites would be catalytically significant as in the case of typical homogeneous catalysts,³² but would retain the beneficial characteristics of a heterogeneous catalyst. In this regard, the **3**/ZrS system was found to have a relatively high active site count, $\sim 65\%$,⁶ versus $\sim 12\%$ for **3**/DA.^{3f}

Titration of an H_2O poison solution was carried out during slurry benzene hydrogenation experiments using the present **3**/AIS catalyst system. From previous protonolytic reactivity studies (including those utilizing isotopic labeling) of chemisorbed zirconium hydrocarbyls,^{4e,f,h} we infer that the present poisoning process involves rapid, catalyst-deactivating cleavage of $\text{Zr-H}/\text{Zr-R}$ bonds with concomitant release of $\text{H}_2/\text{R-H}$. This reactivity pattern is also in accord with well-documented

(29) Tashiro, T.; Sasaki, S.; Kobayashi, M. *Macromolecules* **1996**, *29*, 7460–7469 and references therein.

(30) Bouart, M. *J. Mol. Catal. A* **1985**, *30*, 27–37.

(31) (a) Ittel, S. J. *J. Macromol. Sci., Chem.* **1990**, *A27*, 1133–46. (b) Tait, P. J. T.; Awdza, J. A. M. In *Organometallic Catalysts and Olefin Polymerization: Catalysts for a New Millennium*; Blom, R., Follestad, A., Rytter, E., Tilset, M., Ystenes, M., Eds.; Springer-Verlag: Berlin, 2001; pp 414–426.

(32) Experimental evidence is beginning to suggest that even homogeneous catalysts do not have perfect activation: (a) Liu, Z.; Somsok, E.; Landis, C. R. *J. Am. Chem. Soc.* **2001**, *123*, 2915–2916. (b) Liu, Z.; Somsok, E.; White, C. B.; Rosaaen, K. A.; Landis, C. R. *J. Am. Chem. Soc.* **2001**, *123*, 11193–11207.

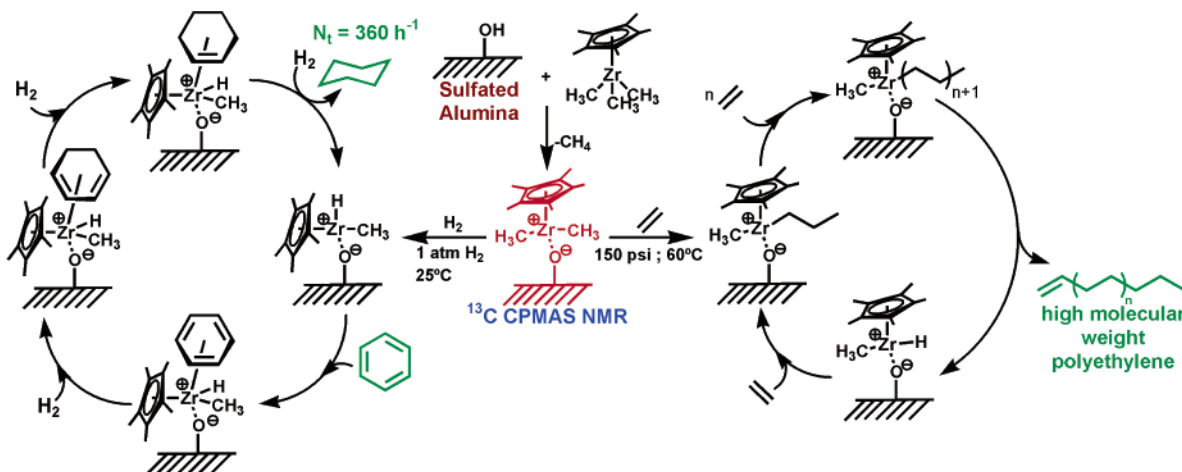


Figure 4. Catalytic pathways for benzene hydrogenation and ethylene polymerization mediated by 3/AIS derived species.

solution phase characteristics of such cationic hydrocarbyls.^{2,6} That the stoichiometrically excess quantities of hydrocarbyl used in the chemisorption process have doubtlessly consumed the great bulk of the accessible AIS acid sites argues that little water is captured/inactivated in acid–base reactions with AIS.

Figure 2 shows the linear response achieved by plotting measured hydrogenation turnover frequency versus the percentage of sites poisoned and making the reasonable assumption at the present Zr coverage (~ 0.25 Zr/nm²) that each H₂O molecule deactivates a single active site. Estimating the zero turnover frequency point by extrapolation reveals that $97 \pm 2\%$ of Zr sites are catalytically significant. Parallel batch poisoning studies for benzene hydrogenation are in excellent agreement and show that $97 \pm 3\%$ of sites are catalytically significant (Figure S1). Carrying out the same batch experiment using ethylene polymerization as the test reaction for the 3/AIS catalyst system reveals that $87 \pm 3\%$ of the Zr sites are significant. The linear response of polymerization activity to poison is shown in Figure 3. The results of this experiment were also duplicated using monoprotic neopentyl alcohol as the poison (Figure S2). The results are equivalent, demonstrating that regardless of the molecular size of the poison or proton content, one poison molecule reacts with/poisons one active site.

Importantly, these results show that the same sites are active for arene hydrogenation and ethylene polymerization, that nearly all of these organozirconium sites are catalytically significant, and that they are directly derived from those cationic species observed in the ¹³C CPMAS NMR.

Conclusions

The present contribution demonstrates through ¹³C CPMAS NMR techniques employing a ¹³C_α-enriched model complex that highly electrophilic, cationic organozirconium species are

formed chemisorptively on a relatively simple, alumina-derived strongly Brønsted acidic surface, sulfated alumina (AIS). In analogy to the surface chemistry of the model complex on DS and DA, and known model compounds in solution, highly electrophilic “cation-like” organozirconium structures are formed on the AIS surface via a Zr-hydrocarbyl protonolytic pathway – a very different reaction mode than that (alkide abstraction) which gives rise to similar cationic species on dehydroxylated alumina. The conclusions of this structural study are supported by the appreciable benzene hydrogenation and ethylene homopolymerization activities of the supported catalysts. Additionally, kinetic active site poisoning experiments show that $\sim 97\%$ of the Zr sites are catalytically significant in 3/AIS-mediated benzene hydrogenation and $\sim 87\%$ active in 3/AIS-mediated ethylene polymerization. Such high populations of catalytically significant sites are, to our knowledge, unprecedented and also reveal that the same sites are active for these very different transformations (or at least derive from a common intermediate). Furthermore, the spectroscopy demonstrates that the cationic organozirconium species observed in the ¹³C CPMAS NMR is indeed the precursor to the catalytically active sites. These relationships are summarized in Figure 4.

Acknowledgment. We are grateful to the Division of Chemical Sciences, Office of Basic Energy Research, U.S. Department of Energy, for support of this research under Grant DE-FG02-86ER13511.

Supporting Information Available: Figures S1 and S2 (PDF). This material is available free of charge via the Internet at <http://pubs.acs.org>.

JA0212213